Energy Efficient Timing Synchronizer for MB-OFDM UWB

Debarati Sen, *Member, IEEE*, Saswat Chakrabarti, *Member, IEEE,* and R. V. Raja Kumar, *SM, IEEE*

***Abstract*— A cross-correlation function (CCF) based timing synchronization algorithm of low complexity, applicable for single-band transmission is presented. Novelty of the synchronizer lies in utilization of specific preamble structure of the Multi-band OFDM frame format. This threshold based algorithm also takes care of the fact that stronger multipath components frequently appear on the later clusters. Performance of the algorithm is measured in terms of mean-squared-error and synchronization probability. Performance is compared with another single-band based timing algorithm by Yak *et al.* [2]. The probability of correct detection is analyzed mathematically to verify the experimental results.**

***Index Terms*— Timing Synchronization; MB-OFDM; UWB**

I. Introduction

FOR Multi-band Orthogonal Frequency Division Multiplexing (MB-OFDM) based Ultra-Wideband (UWB) systems, timing synchronization at the receiver is an important issue. Timing synchronization is divided into: 1) symbol timing synchronization, 2) sampling clock synchronization. Here we focus on symbol timing synchronization to find an estimate of where the fast Fourier transformation (FFT) window starts. Inaccurate symbol timing introduces Inter-Carrier-Interference (ICI), Inter-Symbol-Interference (ISI), affects the quality of channel estimation and signal energy.

ECMA-368 [1] for MB-OFDM offers ten different time-frequency codes for hopping OFDM symbols over multiple bands. This provides transmit diversity and accommodates several UWB devices with minimal interference from each other. These hopping patterns can be classified into: time-frequency interleaved (TFI) and fixed frequency interleaved (FFI) patterns. In FFI transmission, symbols are transmitted in any particular band following a predefined FFI pattern. We refer this as 'single-band based transmission' where the whole packet/frame synchronization (FS/PS) block of the preamble i.e. 24 OFDM symbols are available in a single-band. This helps to design a low-complexity timing synchronizer with a provision to combat typical characteristics of UWB channel. Investigating all schemes in literature, we propose a new cross-correlation function (CCF) based timing synchronizer.

Rest is as follows: Section II discusses the new timing synchronizer. Section III & IV derive its computational complexity and mathematical analysis on probability of correct detection. Section V shows its performance and compares with another algorithm [2]. Summary is given in Section VI.

Debarati Sen is presently with the Department of Signals and Systems, Chalmers University of Technology, Sweden (phone: +46 31 772 1885; e-mail: debarati@chalmers.se). During this work she was associated with the G.S.S.S.T., Indian Institute of Technology Kharagpur, India.

Saswat Chakrabarti is with the G. S. S. School of Telecommunications, Indian Institute of Technology Kharagpur, India.

R. V. Raja Kumar is presently with the R. G. University of Knowledge Technologies, India. During this work he was associated with the Department of E&ECE, Indian Institute of Technology Kharagpur, India.

II. Proposed Timing Synchronization Algorithm

We present a CCF based symbol timing synchronization algorithm applicable for single-band transmission for MB-OFDM UWB. UWB channel impulse response (CIR) does not exhibit a single exponential decay like narrow-band fading channel. Stronger component may not occur in the first cluster, instead, found in later clusters because of the wide bandwidth involved. Sometimes cluster shape does not show a sharp onset, but it shows a gradual increase until a local maximum is reached and then decreases [3]. So, a correlation peak based timing algorithm like Schmidl *et al.* [4] is unsuitable as the timing metric here is based on signal strength of the multipath component which may give false lock and wrong estimation. Algorithm by Van De Beek *et al.* [5] utilizes correlation with cyclic prefix (CP) is also unsuitable as symbols are designed with zero padded (ZP) prefix instead of CP.

Our algorithm considers these features to find the symbol timing. To extract timing information from a communication link, one needs to locate the first significant multipath (FSM) even in presence of dense multipath. Our algorithm attempts to determine FSM by comparing difference of CCF with a predefined threshold. Next, we describe the detailed algorithm.

A. The Proposed Timing Algorithm

MB-OFDM preamble bears a clear demarcation between the first 21 OFDM symbols (PS) and the last 3 OFDM symbols (FS) in the PS/FS block as FS symbols are 180° out of phase w.r.t. PS symbols. Our algorithm utilizes this in finding the symbol timing. Hence, it is a timing algorithm that focuses on boundary detection. It utilizes the cross-correlation function to estimate timing at sample level precision. It yields good system performance and found computationally intensive.

Let, $\{S\}$ denotes a modulated sequence transmitted over time-dispersive UWB fading channel as

$$S = \{.....s(n), s(n+1), ...\} \quad (1)$$

Let, $\{h_b\}$ be the complex base band equivalent UWB channel coefficients for band 'b' with order P as

$$h_b = \{h_b(1), h_b(2), ..., h_b(P)\} \quad (2)$$

Let, $\{\tilde{Y}\}$ be the corresponding received complex sample sequence at UWB receiver front end as

$$\tilde{Y} = \{....., y(n), y(n+1), ...\} \quad (3)$$

We define 'L' as the total number of MB-OFDM symbols each denoted by 'N_s' samples in a transmitted preamble. The n-th received sample of l-th OFDM symbol $y(l,n)$ is as

$$y(l,n) = \sum_{p=1}^{P} s(l, n-p-q) h_b(p) + w(l,n);\ 0<n<N,\ 0<l<L,\ 1\le p\le P \quad (4)$$

where, $w(l,n)$ is the complex additive white Gaussian noise (AWGN) associated with n-th sample of l-th symbol and q is timing offset. Assuming that packet detection is over, our algorithm estimates the start of the first FS sequence and hence computes the start of FFT window for it. Let us define: $n_{correct}$ is starting sample of FFT window, $\hat{n}$ = estimated timing instant

of $n_{correct}$. Received samples are cross-correlated with known training sequences i.e. preamble pattern $\{t\}=\{t(1),t(2),...,t(N)\}$ and the output of n-th sample of l-th symbol $C(l,n)$ is

$$C(l,n)=\sum_{i=1}^{N} y(l,n+i)t^{*}(i) \text{ for } 1\le l\le L;\ 1\le n\le N_s \quad (5)$$

where, * denotes complex conjugate operation. Next, each received sample given by Eq. (5) is subtracted from corresponding sample of (l-1)-th symbol. The difference is as

$$D(n)=C(l,n)-C((l-1),n) \text{ for } 2\le l\le L \quad (6)$$

When both correlated samples belong to different polarity $D(n)$ increases; and at same polarity $D(n)$ gives associated noise magnitude. When received sequence is aligned with first sample of FFT window, $D(n)$ have a magnitude. The algorithm normalizes absolute $D(n)$ with its maximum. So we can say

$${}_{N}D(n)=\left|D(n)\right|/\max\left(\left|D(n)\right|\right) \quad (7)$$

The difference outputs are compared with a predefined threshold 'λ'. If the normalized value ${}_{N}D(n)$ exceeds 'λ', initial timing estimation point $\hat{n}$ is set at 'n' given as

$$\hat{n}=n\Big|_{{}_{N}D(n)\ge\lambda} \quad (8)$$

The actual start of the FFT window is then computed as

$$n_{sync}=\hat{n}+N_s \quad (9)$$

Fig. 1 shows flow diagram of our algorithm. Each received sample is cross-correlated with known sequence $\{t\}$ and stored in a buffer. Next, it checks if the received sample index is higher than N_s. It continues to collect and correlate the received samples till $n<N_s$. It evaluates difference of samples which are 1 OFDM symbol apart. Difference normalized to its maximum is next compared against λ. It is expected to cross the threshold when opposite polarity samples of FS sequence start arriving. The start of FFT window is estimated by shifting the sample index where difference crosses λ by N_s. The functional blocks are detailed through the Eq. (4) to (9). Next, we calculate computational complexity of the synchronizer.

III. Computational Complexity of New Synchronizer

Computational complexity is assessed in terms of equivalent floating point operations (FLOP) needed to carryout timing estimation. Our algorithm performs following operations: a) conjugate multiplication of N samples with known training sequence, b) check if the sample index is ≥ total samples in 1 symbol (N_s), c) compute difference of 2 samples at 1 OFDM symbol apart, d) find maximum difference value, e) normalize difference obtained, f) compare normalized difference with λ. As our algorithm detects boundary of uniform phase and out of phase in PS/FS block, total 22 symbols are involved in it.

We define: T_{OFDM} = time period of 1 OFDM symbol. To obtain timing information we do 3 operations: compute CCF; take difference of correlated output and normalize; find instant when difference envelope crosses λ. CCF computation needs $22N_sN$ and $22N_s(N\text{-}1)$ complex multiplications and additions. To find if n crosses N_s, we do N_s complex addition. Difference computation of 2 samples requires $21N_s$ complex additions. We assume that division is trivial. To find timing instant when difference envelope exceeds λ, we do $20N_s$ additions. To find exact start of FFT window 1 more addition is required.

Thus, total numbers of multiplication involved is

$$\left(N_S N\right)/T_{OFDM} \ \textit{multiplications/sec} \quad (10)$$

Similarly, total numbers of necessary addition operation is

$$\frac{22N_S(N-1)+N_s+21N_s+20N_s}{22T_{OFDM}}=\frac{N_S(N+0.91)}{T_{OFDM}} \ \textit{additions/sec} \quad (11)$$

In comparison, FTA algorithm [2] requires $\{N_S(N+0.95)\}/T_{OFDM}$ multiplications and additions per second. So, our algorithm promises 4% reduction in computational complexity compared to FTA. Also, it achieves improved MSE and synchronization probability in comparison to [2] as will be shown in Section V. Next, we derive the correct timing detection probability.

IV. Determining Correct Timing Detection Probability

To understand the performance of a MB-OFDM system with synchronization, we provide the BER analysis of a convolution coded system. It captures the log-normal fading statistics of channels and considers estimation error variances of timing and CFO estimation by our earlier proposed synchronizers[1] ATS [6]-[7] and MBAFS [8]-[9] respectively. By invoking moment generating function (MGF) and using Gauss-Hermite quadrature integration, average BER for rate R_{cc} coded QPSK modulation with ATS and MBAFS, and channel estimation by least square method is obtained. Analysis is validated through simulation results.

During initial acquisition of an OFDM symbol successive decisions are taken to reach time alignment between received sequence and locally generated sequence. The process of acquisition depends on detection of λ. We analyze probability of correct timing detection in log-normal fading UWB channels at a given SNR for non-coherent data detection.

We consider $p\left(t+\xi T_S\right)$ as a training sequence of length L_S samples transmitted over $L_S \times T_S$ seconds. Here, ξT_S is the delay of the training sequence w.r.t. chosen time sequences. Let $y(t)$, received signal at receiver front end, be given as

$$y(t)=\sqrt{2S}p\left(t+\tau T_S\right)\cos\left(\omega_0 t+\omega_d t+\theta\right)+n(t) \quad (12)$$

where, ω_0 = carrier frequency (radian); ω_d = Doppler radian frequency; θ = carrier phase (random); $n(t)$ = AWGN with two sided power spectral density of $N_0/2$; S = transmitted signal power. Usually, in WPAN, ω_d is very small. Major problem is to align unknown timing τT_S of received signal with known timing ξT_S of the local identical code generator in receiver. Thus alignment should be within 'one chip-interval' such that the absolute timing offset normalized to T_S, $|\psi|=|\xi-\tau|$ is < 1. Performing this operation implies that timing acquisition is achieved. Let us consider following hypotheses:

H_1 : positive synchronization or a 'hit' such that $|\psi|<1$.

H_0 : negative synchronization with condition that $|\psi|\ge 1$.

[1] Because of page limitation, readers are requested to follow reference [6]-[7] and [8]-[9] for our earlier proposed timing and frequency synchronizers ATS and MBAFS respectively.

Our analysis is on positive synchronization. Timing detection is done by envelope threshold comparison between H_0 and H_1. Polydoros *et al.* [10] says that this comparison is equivalent to composite maximum likelihood ratio test between H_0 and H_1. The term 'composite' comes due to the timing uncertainty associated. Now, the in-phase and quadrature-phase variables e_i and e_q can be written after base band conversion and correlation with known training sequence at receiver end as

$$e_i = x\cos\theta + n_i;\quad e_q = x\sin\theta + n_q \tag{13}$$

where, θ is uniformly distributed in (0, 2π); n_i and n_q are independent and identically distributed (i.i.d.) zero mean Gaussian random noise of variance σ_n^2 so as $\sigma_n^2 = N_0 M T_S/2$; MT_S is correlation time; x is output of correlation of received sequence with known training sequence. Now, x may be as

$$x = \sqrt{S}\int_0^{MT_S} p\left(t+\xi T_S\right) p\left(t+\tau T_S\right) dt \tag{14}$$

Also, outcome of correlation is a random variable written as

$$x = \overline{x} + x^{rand} \tag{15}$$

wherein, $\overline{x}$ and x^{rand} are the mean and random part of x greatly depend upon specific code sequence. For mathematical tractability and ease of presentation, we list below the assumptions made in deriving the right detection probability.

***Assumptions* :**

1. The training sequence $p(t)$ has a period $L_S >> 1$.

2. We rewrite timing offset ψ as sum of integer number of timing shifts ψ' and a residual offset of ψ'' as $\psi = \psi' + \psi''$.

3. ψ'' is uniformly distributed in (-1, 1).

4. The correlation length M >> 1.

The mean $\overline{x}$ conditioned on ψ'' and H_i (where, i = 0, 1) can be shown as auto-correlation function of $R_C(\psi'')$ [11], [12] as

$$\overline{x} = E\left\{x\middle|_{H_i,\psi''}\right\} = \sqrt{S}MT_S R_c\left(\psi''\right) \tag{16}$$

wherein, $$R_c^i(\psi'') = \begin{cases} 1-|\psi''| & (H_1) \\ 1/L_s & (H_0) \end{cases} \tag{17}$$

The conditional variance is obtained as

$$\mathrm{var}\left\{x\middle|_{H_i,\psi''}\right\} = MT_S\left[ST_S G_i\left(\psi''\right) + \frac{N_0}{2}\right] \tag{18}$$

wherein, $$G_i(\psi'') = \begin{cases} (\psi'')^2 & (H_1) \\ 1-2|\psi''|+2(\psi'')^2 & (H_0) \end{cases} \tag{19}$$

Equation [13] shows for a large class of codes the correlation output x closely resembles Gaussian distribution. We need to detect a Gaussian random variable x in AWGN from Eq. (13). Combining Eq. (16) and (17) the mean and variance of x is as

$$m_i = \sqrt{S}MT_S R_c^i(\psi'') \quad i = 0, 1 \text{ for } H_0 \text{ and } H_1 \tag{20}$$

$$\sigma_i^2 = SMT_S^2 G_i\left(\psi''\right) \tag{21}$$

Defining variance of x as the self noise of correlator, we say total noise variance as, $\sigma^2 = \sigma_i^2 + \sigma_n^2$. We define probability of right detection (P_d) as probability that envelope $R = \sqrt{e_i^2 + e_q^2}$ crosses R_0 w.r.t. H_1. Depending on H_i and x the probability density function of R is Rician distributed shown as

$$f_{H_i}(R|x) = \left(R/\sigma_n^2\right) I_0\left(xR/\sigma_n^2\right)\exp\left\{-\left(\left(x^2+R^2\right)/2\sigma_n^2\right)\right\};\ \mathrm{R}\geq 0 \tag{22}$$

where, I_0 = modified Bessel's function of first kind and 0-th order. Averaging $f_{H_i}(R|x)$ over Gaussian distribution of x

$$f_{H_i}(R) = \int_{-\infty}^{\infty} \frac{\mathrm{R}}{\sigma_n^2} I_0\frac{xR}{\sigma_n^2}\exp\left\{-\frac{x^2+R^2}{2\sigma_n^2}\right\}\frac{1}{\sqrt{2\pi}\sigma_i}\exp\left\{-\frac{(x-m_i)^2}{2\sigma_i^2}\right\}dx;\ \mathrm{R}\geq 0 \tag{23}$$

$$= \frac{\mathrm{R}}{\sigma_n^2}\frac{1}{\sqrt{2\pi}\sigma_i}\exp\left(\frac{-R^2}{2\sigma_n^2}\right)\exp\left(\frac{-m_i^2}{2\sigma_i^2}\right)\int_{-\infty}^{\infty} I_0\left(\frac{xR}{\sigma_n^2}\right)\exp\left\{-\frac{x^2}{2\sigma_n^2}\right\}\exp\left\{-\frac{\left(x^2-2xm_i\right)}{2\sigma_i^2}\right\}dx \tag{24}$$

Substituting $\rho_i = \frac{\sigma_i}{\sigma_n}$ and $\frac{1}{\sigma^2} = \frac{1}{\sigma_n^2} + \frac{1}{\sigma_i^2} = \frac{1}{\sigma_n^2}\left(1+\rho_i^{-2}\right)$ Eq. (24) is as

$$f_{H_i}(R) = \tag{25}$$

$$= \frac{\mathrm{R}}{\sqrt{2\pi}\rho_i\sigma_n^2}\exp\left(\frac{-R^2}{2\sigma_n^2}\right)\exp\left(\frac{-m_i^2}{2\rho_i^2\sigma_n^2}\right)\int_{-\infty}^{\infty} I_0\left(\frac{xR}{\sigma_n^2}\right)\exp\left\{-\frac{1}{2\sigma^2}\left(x^2-\frac{2xm_i}{1+\rho_i^2}\right)\right\}dx$$

It is noticed from the relation $\frac{1}{\sigma^2} \cong \frac{1}{\sigma_n^2} + \frac{1}{\sigma_i^2}$ that $\frac{\sigma^2}{\sigma_i^2} = \frac{1}{1+\rho_i^2}$.

Utilizing this in equation (25) we get

$$f_{H_i}(R) = = \frac{R}{\sqrt{2\pi}\rho_i\sigma_n^3}\exp\left(\frac{-R^2}{2\sigma_n^2}\right)\exp \tag{26}$$

$$\left\{\left(\frac{m_i^2}{2\sigma^2\left(1+\rho_i^2\right)^2} - \frac{m_i^2}{2\rho_i^2\sigma_n^2}\right)\right\}\int_{-\infty}^{\infty} I_0\left(\frac{xR}{\sigma_n^2}\right)\exp\left\{-\frac{1}{2\sigma^2}\left(x-\frac{m_i}{1+\rho_i^2}\right)^2\right\}dx$$

We further substitute

$$I_i(R) = \int_{-\infty}^{\infty} I_0\left(xR/\sigma_n^2\right)\exp\left\{-\left(1/2\sigma^2\right)\left\{x-\left(m_i/\left(1+\rho_i^2\right)\right)\right\}^2\right\}dx \tag{27}$$

which finally leads to simplified expression for $f_{H_i}(R)$ as,

$$f_{H_i}(R) = = \frac{\mathrm{R}}{\sqrt{2\pi}\rho_i\sigma_n^3}\exp\left(\frac{-R^2}{2\sigma_n^2}\right)\exp\left\{\frac{-m_i^2}{2\sigma_n^2\left(1+\rho_i^2\right)}\right\}I_i(R);\ \mathrm{R}\geq 0 \tag{28}$$

For hypothesis H_1 (probability of right detection) mean m_1 and variance σ_1^2 of correlated output x is as

$$m_1 = \sqrt{S}MT_S R_c^1\left(\psi''\right) \quad (29);\qquad \sigma_1^2 = SMT_S^2 G_1\left(\psi''\right) \tag{30}$$

Hence, the expression (27) for H_1 hypothesis becomes

$$I_1(R) = \int_{-\infty}^{\infty} I_0\left(xR/\sigma_n^2\right)\exp\left\{-\left(1/2\sigma^2\right)\left\{x-\left(m_1/\left(1+\rho_1^2\right)\right)\right\}^2\right\}dx \tag{31}$$

Instead of obtaining closed form solution, we settle for a series expansion of function $I_0(.)$ using expansion series of modified Bessel's function of first kind [14] as noted below:

$$I_0\left(xR/\sigma_n^2\right) = \sum_{k=0}^{\infty}\left[\left(xR/\sigma_n^2\right)^k \Big/ 2^k\left(k!\right)\right]^2 \tag{32}$$

Now, substituting equation (31) with (32) we get

$$I_1(R) = \sum_{k=0}^{\infty}\left\lfloor\frac{R}{\sigma_n}\right\rfloor^{2k}\left\{\frac{1}{4^k(k!)^2}\right\}\int_{-\infty}^{\infty}(x/\sigma_n)^{2k}\exp\left\{-\frac{1}{2\sigma^2}\left\{x-\frac{m_1}{1+\rho_1^2}\right\}^2\right\}dx \quad (33)$$

On further substitution of $1/\sigma^2 = \left(1+\rho_1^{-2}\right)/\sigma_n^2$ in equation (33)

$$I_1(R) = \sum_{k=0}^{\infty}\left\lfloor\frac{R}{\sigma_n}\right\rfloor^{2k}\frac{1}{4^k(k!)^2}\int_{-\infty}^{\infty}\left(\frac{x}{\sigma_n}\right)^{2k}\exp\left\{-\frac{\left(1+\rho_1^2\right)}{2\rho_1^2}\left(\frac{x}{\sigma_n}-\frac{m_1}{\sigma_n\left(1+\rho_1^2\right)}\right)^2\right\}dx \quad (34)$$

Now, substituting $x/\sigma_n = z$ and $m_1/\left\{\sigma_n\left(1+\rho_1^2\right)\right\} = m_n$ we get

$$I_1(R) = \sum_{k=0}^{\infty}\left\lfloor\frac{R}{\sigma_n}\right\rfloor^{2k}\frac{\sigma_n}{4^k(k!)^2}\int_{-\infty}^{\infty}z^{2k}\exp\left\{-\frac{\left(1+\rho_1^2\right)}{2\rho_1^2}\left(z-m_n\right)^2\right\}dz \quad (35)$$

On further substitution as below

$$\frac{1}{2^k(k!)^2}\frac{1}{\sqrt{2\pi}}\sqrt{1+\rho_1^{-2}}\int_{-\infty}^{\infty}z^{2k}\exp\left\{-\frac{\left(1+\rho_1^2\right)}{2\rho_1^2}\left(z-m_n\right)^2\right\}dz = F_k^* \quad (36)$$

Expression for Bessel's function for H_1 given as $I_1(R)$ is as

$$I_1(R) = \sum_{k=0}^{\infty}\left[R/\sigma_n\right]^{2k}\sigma_n\left\{\sqrt{2\pi}\Big/\left(2^k\sqrt{1+\rho_1^{-2}}\right)\right\}F_k^* \quad (37)$$

Plugging Eq. (37) in (28) probability density function of R is

$$f_{H_1}(R) = \frac{\mathrm{R}}{\sqrt{1+\rho_1^2\sigma_n^2}}\exp\left\{-\frac{R^2}{2\sigma_n^2}\right\}\exp\left\{-\frac{m_1^2}{\left(1+\rho_1^2\right)\left(2\sigma_n^2\right)}\right\}\sum_{k=0}^{\infty}\left\lfloor\frac{R^2}{2\sigma_n^2}\right\rfloor^k F_k^* \quad (38)$$

Probability (P_d) that envelope R goes above threshold R_0 is as

$$P_d = \int_{R_0}^{\infty}f_{H_1}(R)\,dR = \quad (39)$$

$$\frac{1}{\sqrt{1+\rho_1^2}}\frac{1}{\sigma_n^2}\exp\left\{-\frac{1}{2\sigma_n^2}\frac{m_1^2}{\left(1+\rho_1^2\right)}\right\}\int_{R_0}^{\infty}R\exp\left\{-\frac{R^2}{2\sigma_n^2}\right\}\sum_{k=0}^{\infty}\left\lfloor\frac{R^2}{2\sigma_n^2}\right\rfloor^k F_k^* dR$$

Changing order of summation and integration in Eq. (39)

$$P_d = \frac{1}{\sqrt{1+\rho_1^2}}\exp\left\{-\frac{1}{2\sigma_n^2}\frac{m_1^2}{\left(1+\rho_1^2\right)}\right\}\sum_{k=0}^{\infty}F_k^*\int_{R_0}^{\infty}\frac{R}{\sigma_n^2}\exp\left\{-\frac{R^2}{2\sigma_n^2}\right\}\left\lfloor\frac{R^2}{2\sigma_n^2}\right\rfloor^k dR \quad (40)$$

Changing the variable of integration with $\left(R^2/2\sigma_n^2\right) = q$ and $\lambda = \left(R_0^2/\sigma_n^2\right)$, P_d is expressed as

$$P_d = \left(1/\sqrt{1+\rho_1^2}\right)\exp\left\{-\left(1/2\sigma_n^2\right)\left\{m_1^2/\left(1+\rho_1^2\right)\right\}\right\}\sum_{k=0}^{\infty}F_k^*\int_{\lambda/2}^{\infty}q^k\exp(-q)\,dz \quad (41)$$

On further substitution of

$$G_k^* = \int_{\lambda/2}^{\infty}q^k\exp(-q)\,dq \quad (42)$$

On simplification, right detection probability (P_d) is as

$$P_d = \left(1/\sqrt{1+\rho_1^2}\right)\exp\left\{-\left(1/2\sigma_n^2\right)\left\{m_1^2/\left(1+\rho_1^2\right)\right\}\right\}\sum_{k=0}^{\infty}F_k^*G_k^* \quad (43)$$

We derive detailed expressions for coefficients G_k^* and F_k^* next. To relate G_k^* and G_{k+1}^*, we rewrite G_k^* as

$$G_k^* = (\lambda/2)^k\exp(-\lambda/2) + k\underbrace{\int_{\lambda/2}^{\infty}q^{k-1}\exp(-q)\,dq}_{G_{k-1}^*} \quad (44)$$

i.e. $G_{k+1}^* = \left(\lambda/2\right)^{k+1}\exp\left(-\lambda/2\right) + (k+1)G_k^*$ (45); where, $G_0^* = \exp\left(-\lambda/2\right)$ (46)

Similar relation between F_k^* and F_{k+1}^*. So, Eq. (36) is as

$$F_k^* = \frac{1}{2^k(k!)^2}\frac{1}{\sqrt{2\pi}}\sqrt{1+\rho_1^{-2}}\int_{-\infty}^{\infty}z^{2k}\exp\left\{-\frac{1}{2\rho_1^2/1+\rho_1^2}\left(z-m_n\right)^2\right\}dz \quad (47)$$

Now, coefficient F_k^* can be related to non-central moments of a Gaussian distribution $\mathbb{Q}_n(\mu,\sigma^2)$ where

$$\mathbb{Q}_n\left(\mu,\sigma^2\right) = \left(1/\sqrt{2\pi\sigma^2}\right)\int_{-\infty}^{\infty}a^n\exp\left\{-\left(1/2\sigma^2\right)(a-\mu)^2\right\}da \quad (48)$$

Now, F_k^* in terms of Gaussian distribution may be given as

$$F_k^* = \left\{1/\left(2^k(k!)^2\right)\right\}\mathbb{Z}_{2k}\left(m_n,\rho_1^2/1+\rho_1^2\right) \quad (49)$$

Using integration by parts, it can also be shown that $\mathbb{Q}_n(\mu,\sigma^2)$ follows a recursion given as

$$\mathbb{Z}_{n+1}\left(m,\sigma^2\right) = \sigma^2 n\mathbb{Z}_{n-1}\left(m,\sigma^2\right) + m\mathbb{Z}_n\left(m,\sigma^2\right) \quad (50)$$

with initial conditions $\mathbb{Z}_0(m,\sigma^2) = 1$ and $\mathbb{Z}_1(m,\sigma^2) = m$. Using Eq. (49) and (50) we can establish a recursive relation for calculating F_{k+1}^* from F_k^* as

$$F_{k+1}^* = \frac{\left(\rho_1^2/1+\rho_1^2\right)k}{2^k(k+1)^2(k!)^2}\mathbb{Z}_{2k-1}\left(m_n,\frac{\rho_1^2}{1+\rho_1^2}\right) + \frac{m_n}{2^k\,2(k+1)^2(k!)^2}\mathbb{Z}_{2k}\left(m_n,\frac{\rho_1^2}{1+\rho_1^2}\right) \quad (51)$$

To simplify equation (51), we substitute

$$\sigma_*^2 = \left(1/\left(1+\rho_1^2\right)\right)\left(\rho_1^2/\left(1+\rho_1^2\right)\right) = \left(1/\left(1+\rho_1^2\right)\right)\left(2SNR_e^1/\left(1+2SNR_e^1\right)\right) \quad (52)$$

wherein, SNR_e^1 is the effective SNR for hypothesis H_1 given as $SNR_e^1 = \left\{\mu_{final,CM}\tilde{E}_sG_1(p")\right\}/N_0$; $\tilde{E}_S$ is signal power over unit sample time T_S; $\mu_{final,CM}$ is the scaling factor. Further $E_S = \mu_{final,CM}\tilde{E}_sG_1(p")$. Substituting Eq. (52) in (51) we get

$$F_{k+1}^* = \sigma_*^2\frac{k}{(k+1)^2}\frac{\mathbb{Z}_{2k-1}\left(m_n,\frac{\rho_1^2}{1+\rho_1^2}\right)}{2^k(k!)^2} + \frac{m_n}{2(k+1)^2}\frac{\mathbb{Z}_{2k}\left(m_n,\frac{\rho_1^2}{1+\rho_1^2}\right)}{2^k(k!)^2} + \sigma_*^2\frac{k\rho_1^2}{(k+1)^2}\frac{\mathbb{Z}_{2k-1}\left(m_n,\frac{\rho_1^2}{1+\rho_1^2}\right)}{2^k(k!)^2} \quad (53)$$

Let us define $\left\{\left\{\mathbb{Z}_{2k-1}\left(m_n,\left(\rho_1^2/\left(1+\rho_1^2\right)\right)\right)\right\}/2^k(k!)^2\right\} = E_k^*$ (54)

Now, substituting values of E_k^* and F_k^* from Eq. (54) and (49) in Eq. (53) we get simplified expression for F_{k+1}^* as

$$F_{k+1}^* = \sigma_*^2\frac{k}{(k+1)^2}E_k^* + \frac{m_n}{2(k+1)^2}F_k^* + \sigma_*^2\frac{k}{(k+1)^2}\rho_1^2E_k^*;\ F_0^* = 1 \quad (55)$$

It is observed after substituting Eq. (45) and (55) in Eq. (43) that for H_1, $P_d \propto (\lambda$, Effective received SNR). The effective received SNR is dependent on $\mu_{final,CM}$ of operating UWB CM and it varies largely from CM1–CM4. For CM3 and CM4 effective received SNR is found decreasing significantly compared to low dispersive channels ($\mu_{final,CM1} > \mu_{final,CM4}$). This leads to: a) for high dispersive CMs P_d decreases

significantly and to achieve acceptable detection probability, λ needs to increase; b) for low SNR operation, to achieve P_d compatible to high SNR operations λ should be increased.

V. Simulation Results and Discussions

A. Simulation Environment

The algorithm is tested using FFI patterns with time-frequency codes 5, 6, 7 and TFI pattern 1 [1]. To compare our algorithm with FTA [2], we take representative results on its performance with TFI pattern 1. Simulation is carried out for 320 Mbps MB-OFDM system. UWB devices work at low SNR region in practice. So, we test for different SNR of 17, 10, 5 dB, for CM1 and CM2. For CM3 and CM4 we test for high SNR. For each λ, we consider 1000 noisy realizations for each of 100 UWB channels. λ is shown as % of $\max\left({}_N D(n)\right)$.

B. Performance Metric of the Algorithm

Performance is measured by mean-squared-error (MSE) of the estimation and probability of synchronization (P_{sync}) which is equivalent to P_d (Section IV). Table I shows simulated results of MSE and P_{sync} with different λ values for CM1 for noiseless condition and 17 dB SNR. We also consider above parameters at different λ for CM1 for 10 dB SNR. Performance of both with change of λ at 17 dB SNR in CM3 and CM4 is also done.

1) Mean-Squared-Error (MSE)

We define MSE as $$MSE = \sum_{\forall \hat{n}} (\hat{n} - n_{correct})^2 P(\hat{n}) \quad (56)$$

here, $P(\hat{n})$ is probability to estimate $n_{correct}$ at $\hat{n}$. Table I shows CM1 causes a minimum MSE of '0.32' and '0.49' sample for λ of 3% and 5.4% under noiseless condition and 17 dB SNR respectively.

We use a fixed λ based on extent of interfering energy. We find that MSEs for CM1 reach minimum value of '0.52' samples for SNR of 10 dB with λ of 11.7%. For CM2, we find minimum MSE of '10.01' samples at 10 dB SNR. At 17 dB SNR, the highly dispersive CM3 and CM4 show minimum MSE of '16.89' and '25.30' samples at λ of 9.4% and 11.2%.

2) Synchronization Probability

We define the total synchronization probability $P_{sync,total}$ which includes P_{sync} within ZP region which is ISI free region of 32 samples duration long. If $\hat{n}$ falls within this region, sub-carriers will experience phase rotations only. Phase errors can be rectified by channel equalizer and thus synchronization still considered to be achieved. Thus total P_{sync} here is as

$$P_{sync,total} = P_{ZP} + P_{sync} \quad (57)$$

where, P_{ZP} is the probability of estimating timing instant within the zero padded region and P_{sync} is the probability of estimating timing at $\hat{n} = n_{correct}$. But, we are interested with correct P_{sync}, a higher value of which implies more accurate channel estimate. It is to be noted that P_{sync} is same as P_d.

Table I shows that 2.9% λ give highest P_{sync} of '95%' for CM1 under noiseless condition. With 17 dB SNR, CM1 gives maximum P_{sync} of 94.63% with λ of 4% (approx) where CM2 gives maximum P_{sync} of 80.2% with 6.6% λ. At SNR of 10 dB, we observe maximum P_{sync} of 91.42% and 64.09% with λ of 12.3% for CM1 and 20% for CM2. The CM3 and CM4 achieve maximum synchronization of 74% and 52% respectively at the corresponding λ of 7.5% and 8.7% when operating SNR is 17 dB. The P_{ZP} can be evaluated for each CM by estimating their corresponding delay spreads.

Table II shows MSE and P_{sync} for our scheme and Yak *et al.*'s scheme for CM1 and CM2. Correct P_{sync} with our scheme is compared with $P_{sync,total}$ obtained by FTA [2]. We observe that maximum P_{sync} using our method is much higher than FTA for both CMs. Moreover, for CM2, our algorithm gives less MSE by '1.0' sample than FTA under SNR of 17 dB.

C. Comparative Studies between Analysis and Simulation

We compare between analytical and simulation studies on probability of correct detection of timing instant in CM1 and CM2. We plot the analytical graph w.r.t. SNR following P_d derived in Eq. (43). The respective λ for CM1 and CM2 are set at 3.9% and 6.6% of maximum normalized difference ${}_N D(n)$. Simulation studies show that, at these λ values P_{sync} in respective channel reaches maximum. Fig. 2 shows analytical plot of P_d for CM1. We observe that about 94% correct timing detection probability is obtained at typical SNR of 17 dB in CM1. Interestingly, our simulation studies show that at the same threshold the achievable P_{sync} is 94.63% (Table I).

D. Discussions

Thorough investigation with different threshold (λ) levels for CM1–CM4 shows that a proper selection of λ in different UWB CM is essential to get minimum MSE and maximum P_{sync}. Further, intuitively, the optimum λ need be updated for different SNR values under same UWB CM. It is obvious that, a higher value of P_{sync} and minimum value of MSE are always desired for better channel estimation. The $P_{sync,total}$ with our timing algorithm can be obtained by calculating P_{ZP} in the related CM and summing up with the reported result.

VI. Summary

The proposed algorithm locks the timing instant by comparing the difference of correlation samples for two consecutive symbols with a predefined λ in contrast with the conventional correlation based techniques which find strongest multipath component by finding correlation peak. Results of our algorithm show improvement in synchronization probabilities over the reported results in FTA [2] for CM1 and CM2. It also shows lower MSE for CM2 in 17 dB SNR. Following the trend of performance measuring parameters for CM1 and CM2 at low, medium, high SNR, it can be said that the algorithm gives satisfactory results for UWB CM1 and CM2. To achieve satisfactory results in CM3 and CM4, a corresponding high SNR is required. With the SNR of 17 dB, 74% and 52.5% of channel realizations can be synchronized with our algorithm.

VII. Acknowledgement

We would like to acknowledge funding from VINNOVA within the IKT grant 2007-02930 for publication of this paper.

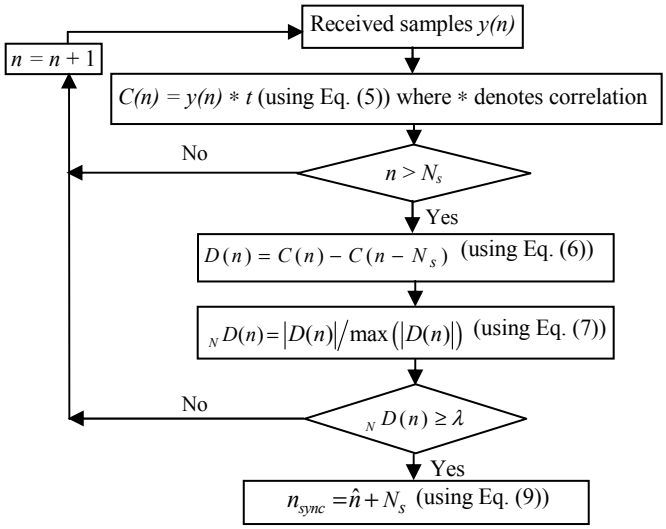

Fig. 1: The proposed Timing Algorithm

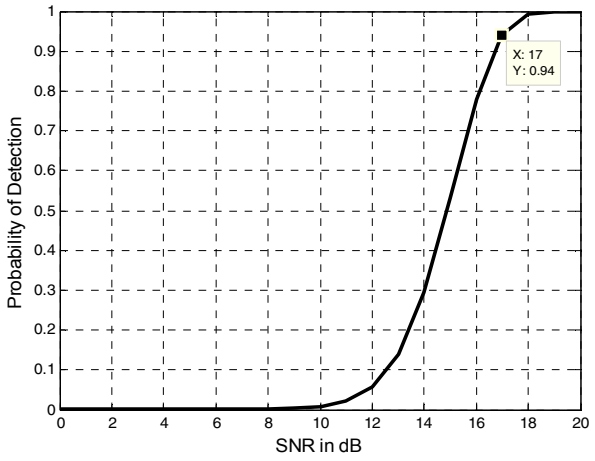

Fig. 2. Probability of detection vs. SNR of proposed algorithm in CM1 at the threshold (λ) of 3.9% of max ($_N D(n)$) from analysis.

TABLE I

MSE AND SYNCHRONIZATION PROBABILITY FOR CM1 IN NOISELESS CONDITION AND 17 DB SNR

λ (%)	**MSE** (sample units)		P_{sync} (%)	
	noiseless	***17dB***	***noiseless***	***17dB***
7.8	0.65	3.38	94.30	89.24
7.5	0.65	1.05	94.20	91.41
7.2	0.63	0.77	94.30	92.00
6.9	0.61	0.65	94.30	92.48
6.6	0.60	0.63	94.20	93.41
6.3	0.60	0.59	94.20	93.59
6.0	0.52	0.55	94.00	93.59
5.7	0.49	0.51	94.00	93.91
5.4	0.43	**0.49**	94.00	94.11
5.1	0.42	0.63	94.00	94.35
4.8	0.42	0.82	95.00	94.46
4.5	0.42	0.93	95.00	94.54
4.2	0.39	1.35	95.00	94.60
3.9	0.39	1.65	95.00	**94.63**
3.6	0.32	2.46	95.00	89.01
3.3	0.32	3.09	95.00	85.83
3.0	**0.32**	3.41	**95.00**	83.17

TABLE II

MSE AND SYNCHRONIZATION PROBABILITY BY OUR TIMING ALGORITHM AND FTA [2] FOR CM1 AND CM2

Perform -ance criterion	**CM1**		**CM2**	
	Proposed Algorithm	***FTA***	***Proposed Algorithm***	***FTA***
MSE, (Min) (samples)	0.32 (noiseless)	0.32 (noiseless)	6.04 (noiseless)	4.02 (noiseless)
	0.49 (17dB)	0.365 (17dB)	**8.13** (17dB)	9.129 (17dB)
Synchroni -zation Probabi -lity (Max)	**95%** (P_{sync}) (noiseless)	85% (P_{sync}) (noiseless)	**86%** (P_{sync}) (noiseless)	55% (P_{sync}) (noiseless)
	94.63% (P_{sync}) (17dB)	81.48% (P_{sync}) (17dB)	**80.23%** (P_{sync}) (17dB)	49% (P_{sync}) (17dB)

REFERENCES

[1] Standard ECMA-368, "High Rate Ultra Wideband PHY and MAC Standard," 3rd Edition, December 2008, <http://www.ecma-international.org/publications/standards/Ecma-368.htm>.

[2] Yak, C. W., Lei, Z., Chattong, S, Tjhung, T. T., "Timing synchronization for ultra-wideband (UWB) multi-band OFDM systems," *IEEE VTC Fall*, Dallas, Texas, USA, vol. 3, pp. 1599–1603, September 25–28, 2005.

[3] Molisch, A. F., "Ultrawideband propagation channels - theory, measurement, and modeling," *IEEE Transactions on Vehicular Technology*, vol. 54, no. 5, pp. 1528–1545, September 2005.

[4] Schmidl, T. M., Cox, D. C., "Robust frequency and timing synchronization for OFDM," *IEEE Transactions on Communications*, vol. 45, no. 12, pp. 1613–1621, December 1997.

[5] Van De Beek, J. J., Sandell, M., Borjesson, P. O., "ML estimation of time and frequency offset in OFDM systems," *IEEE Transactions on Signal Processing*, vol. 45, no. 7, pp. 1800–1805, July 1997.

[6] D. Sen, S. Chakrabarti, R. V. Raja Kumar, "An Energy Based Symbol Timing Synchronization Scheme for MB-OFDM Based Ultra-Wideband Communication," *IEEE ISSSTA*, Italy, pp. 446-451, Aug. 25-28, 2008.

[7] D. Sen, S. Chakrabarti, R. V. Raja Kumar, "A Multi-Band Timing Estimation and Compensation Scheme for Ultra-Wideband Communications," *IEEE Globecom*, USA, pp. 1-5, Nov.30-Dec.04, 2008.

[8] D. Sen, Saswat Chakrabarti, and R. V. Raja Kumar, "An Efficient Frequency Offset Estimation Scheme for Multi-band OFDM Ultra-Wideband Systems," *IEEE VTC Spring*, Singapore, pp. 973-977, May 11-14, 2008.

[9] D. Sen, S. Chakrabarti, R. V. Raja Kumar, "An Improved Frequency Offset Estimation Algorithm by Multi-Band Averaging Method for MB-OFDM based UWB Communication for WPAN Applications," *IEEE ANTS*, Bombay, India, pp. 1-3, Dec.15-17, 2008.

[10] Polydoros, A., Weber, C. L., "Worst-case considerations for coherent serial acquisition of PN sequences," National Telecommunications Conference, Houston, TX, USA, pp. 24.6.1–24.6.5, December 1980.

[11] Golomb, S. W., Shift Register Sequences, Holden Day, San Fransisco, CA, USA, 1967.

[12] Lindholm, J. H., "An analysis of the pseudo randomness properties of subsequences of long M-sequences," *IEEE Transactions on Information Theory*, vol. 53, no. 11, pp. 1269–1273, November 2006.

[13] Bekir, N. E., "Bounds on the distribution of partial correlation for PN and Gold codes," Ph.D dissertation, Dept. of Electrical Engg., Uni. Southern California, LA, USA, January 1978.

[14] Middleton, D., Introduction to Statistical Communication Theory, McGraw-Hill, New York, USA, 1960.